DEPENDENCE OF PORE STRUCTURE ON CURING CONDITIONS AND EVALUATION OF CRITICAL PORE SIZE AFFECTING CARBONATION OF CONCRETE

(Translation from Preceedings of JSCE, No.718/V-57, November 2002)

Doyeon KWAK

Kimitaka UJI

Katsuro KOKUBU

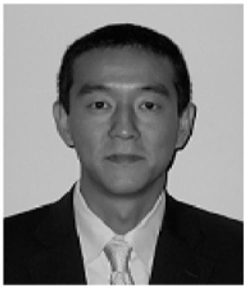

Atsushi UENO

The pore structure of concrete depends on the cement type, curing procedure, and mix proportion, and has a significant influence on the compressive strength, chloride penetration, carbonation rate, and shrinkage properties of a completed structure. Furthermore, the pore structure of the surface and internal layers differs because of early-age drying. The purpose of this study is to investigate variations in pore structure with depth under different curing conditions and their influence on carbonation. Results suggest that the volume of pores larger than 40 nm has a significant influence on carbonation rate, and there is a possibility that carbonation rate can be estimated from the pore structure.

Key Words: *compressive strength, carbonation rate, curing conditions, pore size distribution*

Doyeon KWAK is a doctoral student at Tokyo Metropolitan University where he received his MS in Civil Engineering in 2001. He holds a BS in civil engineering from the University of Seoul, Korea. His research interests include pore structure in concrete and the durability of concrete structures. He is a member of JSCE.

Kimitaka UJI is an associate professor in the Graduate School of Engineering at Tokyo Metropolitan University. He obtained his D.Eng from Yokohama National University in 1993. His research interests include repair and strengthening of concrete structures and construction. He is a member of JSCE.

Katsuro Kokubu is a professor in the Graduate School of Engineering at Tokyo Metropolitan University, Japan. He obtained his doctoral degree from Tokyo Metropolitan University in 1983. He is a member of concrete committee in JSCE and an administrator of JCI. His research interest includes utilization of byproducts as mineral admixtures, slag aggregates and recycled aggregates and compaction of concrete.

Atsushi UENO, a member of JSCE, is a research associate in Graduate School of Engineering at Tokyo Metropolitan University. His research interests relate to the physical interaction between various material particles and liquid phase in concrete.

1. INTRODUCTION

The pore structure of cured concrete depends on a number of factors, including the type of cement used, the curing procedure, and the mix proportion. A nonporous microstructure can only be achieved if appropriate curing conditions are adopted during the initial period of hydration. The standard specifications of the Japan Society of Civil Engineers (JSCE) stipulate that concrete using ordinary portland cement (OPC) should be kept moist for at least five days, while high-early-strength portland cement (HPC) requires at least three days of curing and blended cement (portland blast-furnace slag cement and portland fly-ash cement) should be cured for at least seven days[1]. However, it cannot be expected that such conditions will always be met. As a result, the pore structure of the surface and internal layers will differ due to drying that takes place immediately after demolding[2][3].

Few studies of concrete's microstructural properties have focused on the influence of curing conditions[4]. Recognizing that the physical properties of a material depend on its internal structure, the authors study variations in pore structure with depth in order to investigate the influence of curing conditions and cement type on concrete properties. The development of compressive strength and carbonation is also considered.

A large number of investigations have examined changes in pore structure as carbonation proceeds[5]. However, little is known about the effect of pore size or pore structure on the process of carbonation. Since carbonization requires penetration of carbon dioxide and diffusion inwards from the surface, it requires the presence of capillary voids. Therefore, we can conjecture that there is a critical pore size that will affect the mechanism of carbonation.

In this study, tests of pore size distribution and accelerated carbonation are carried out to investigate the effect of pore structure and pore size on carbonation.

2. EXPERIMENTAL METHOD

2.1 Mix proportions and curing conditions

The materials and mix proportions used in this study are presented in Tables 1 and 2. The cements used were OPC, HPC, and ground granulated blast-furnace slag (BFS) with 50% cement by weight. The cementitious material content and ratio of water to cementitious material were 342 kg/m^3 and 50%, respectively, in all tests.

Molds were removed one day after concrete placement, and the specimens were cured for the designated duration. A total of 13 curing sets were cast: 7 sets for OPC and 3 each for HPC and

Table 1. Properties of materials

Materials	Types	Properties
Binder	Ordinary portland cement	Density : 3.16g/cm^3、Specific surface area : 3320cm^2/g
	High-early-strength portland cement	Density : 3.14g/cm^3、Specific surface area : 4470cm^2/g
	Ground granulated blast-furnace-slag	Density : 2.91g/cm^3、Specific surface area : 4160cm^2/g
Fine aggregate	Crushed sand + Pit sand	Density：2.63g / cm^3、Water absorption：1.47%、 Percentage of absolute volume：64.6%、F.M 2.62
Coarse aggregate	Crushed stone	Density：2.65g /cm^3、Water absorption：0.73 Percentage of absolute volume：61.6%、F.M6.79、 Maximum grainsize：20mm

Table 2. Mix proportions

symbol	W/B (%)	s/a (%)	Unit weight (kg/m³)				
			W	C	BFS	S	G
OPC	50	44.2	171	342	0	786	998
HPC	50	44.2	171	342	0	785	997
BFS	50	44.2	171	171	171	780	991

BFS. All samples were cured for a total of 28 days. Looking at the case of OPC, samples 28A, 28W, and 28S were, respectively, cured in air, water, and sealed conditions for 27 days after demolding (the letter refers to the initial curing method: A = air, W = water, S = sealed; the initial number refers to the period of initial curing in days). Samples 3W28, 5W28, and 7W28 were cured in water for 2, 4, and 6 days followed by 25, 23, and 21 days of curing in air, respectively. These curing conditions are summarized in Fig. 1. For HPC and BFS samples, the curing sets consisted of 3W28, 7W28, and 28W.

Sealed curing was achieved by covering the specimens with food wrapping film and a specially made vinyl. Air and sealed curing took place in a curing room at a temperature of 20 ± 1°C and a relative humidity of 60%. Water curing was carried out at a water temperature of 20 ± 1°C. After the 28 days of curing, accelerated carbonation tests were carried out on the OPC specimens.Compressive strength and pore size distribution tests were performed at 3, 5, 7, and 28 days.

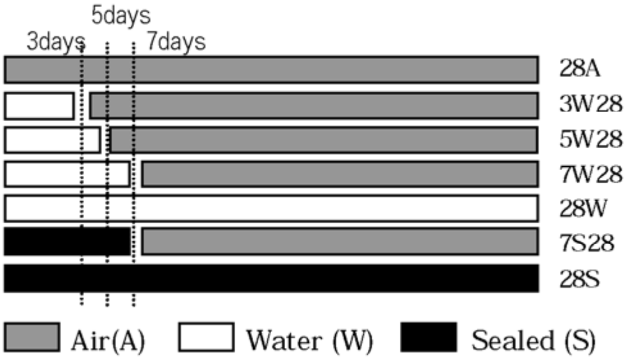

Fig. 1 Curing conditions

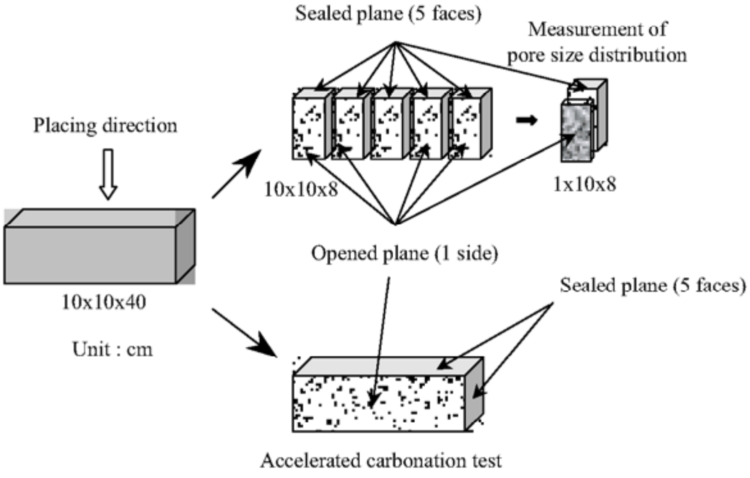

Fig. 2 Specimens preparation

2.2 Experimental methods

a) Compressive strength

Cylindrical specimens with a diameter of 10 cm were used for compression tests. The experiments were carried out in accordance with Japan Industrial Standard JIS A 1108.

b) Carbonation depth

Seven sets of prism-shaped OPC specimens (10 x 10 x 40 cm) were used for accelerated carbonation tests, as shown in Fig. 2. Five of the six faces were coated with epoxy resin and silicon after appropriate wet curing (for 3, 5, 7, and 28 days) in order to expose only one side at all times. All specimens were transferred to a specially built chamber to accelerate the carbonation process after the full 28 days of curing.

The carbonation chamber was maintained at a temperature of 40℃, a relative humidity of 60%, and 7% by volume of carbon dioxide. Testing was performed after specimens had been in the chamber for 4, 12, 24, and 48 weeks. At each test age, a slice measuring approximately 80 mm was split normal to the major axis of the specimen. The shortened specimen was replaced in the chamber and exposure continued. The broken surface of the slice was immediately cleaned and sprayed with a 1% phenolphthalein indicator. The average of the 10 measurements was taken as the carbonation depth at the age of the test.

c) Pore size distribution

As shown in Fig. 2, the specimens used in the pore size distribution tests were prism shaped specimens measuring 10 x 10 x 8 cm. Cutting was performed using a dry cutter after the prescribed period of water curing (3, 5, 7, and 28 days). The specimens were coated with epoxy resin and silicon so as to expose only one face. Measurements were carried out with a mercury porosimetry in the range 6 nm-500 μ m. The sliced specimens (1 x 10 x 8 cm) were crushed into particles measuring 2.5-5 mm and then immersed in acetone to prevent hydration. The pore size distribution was measured after vacuum drying.

3. VARIATION OF PORE STRUCTURE WITH CURING CONDITIONS

3.1 Influence of curing period

Figure 3 shows the variation in pore structure as a function of curing period for OPC concrete cured in water. It can be seen that there is no significant variation with depth at each age, and a homogeneous pore structure is achieved. The total pore volume decreases slightly as the curing period increases. Since cement hydration may be looked upon as a process during which the space originally occupied by cement and water becomes filled with hydration products, it is reasonable that the volume of pores exceeding 50 nm decreases with hydration, while there is an increase in pores smaller than 50 nm. However, the volume of pores above 100 nm does not change as hydration progresses.

The variations in pore size distribution at 3, 5, 7, and 28 days for OPC, HPC, and BFS are presented in Fig. 4 as a cumulative curve. Total pore volume decreases as the period of wet curing is increased, regardless of cement type. The volume of pores larger than 200 nm in OPC and HPC, however, does not change between 3 days and 28 days. The behavior of BFS appears to differ from that of OPC and HPC; this is thought to result from the relatively active hydration of ground granulated blast-furnace-slag up to 7 days[6]. After 7 days, the volume of pores larger than 200 nm in BFS varies little, just as with the other cement types. In summary, the principal variation in pore structure with hydration occurs in pores smaller than 200 nm, and there is no significant reduction in the volume of pores larger than 200 nm. There is a much more conspicuous reduction in the volume of smaller pores.

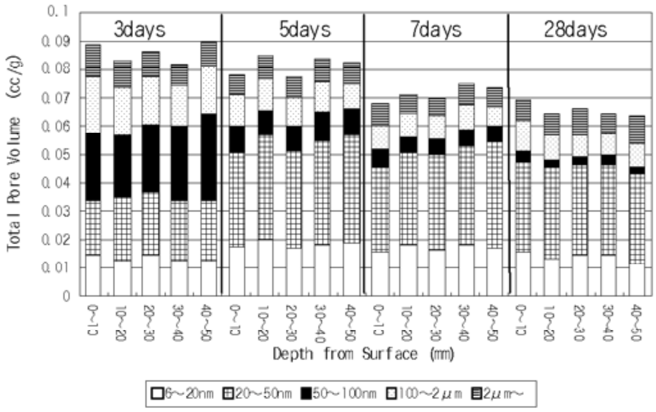

Fig. 3 Variation in pore structure with water curing duration

Figure 3 shows that the volume of

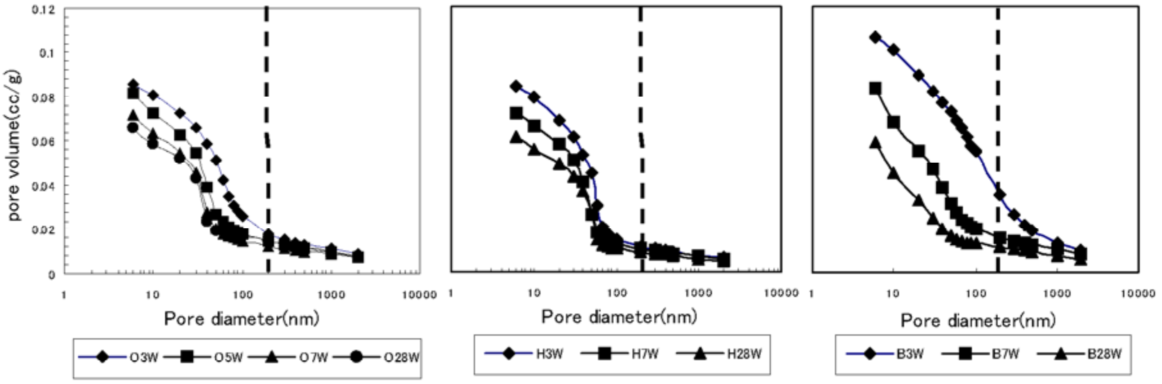

(a) OPC (b) HPC (c) BFS

Fig. 4 Variation in pore size distribution with hydration

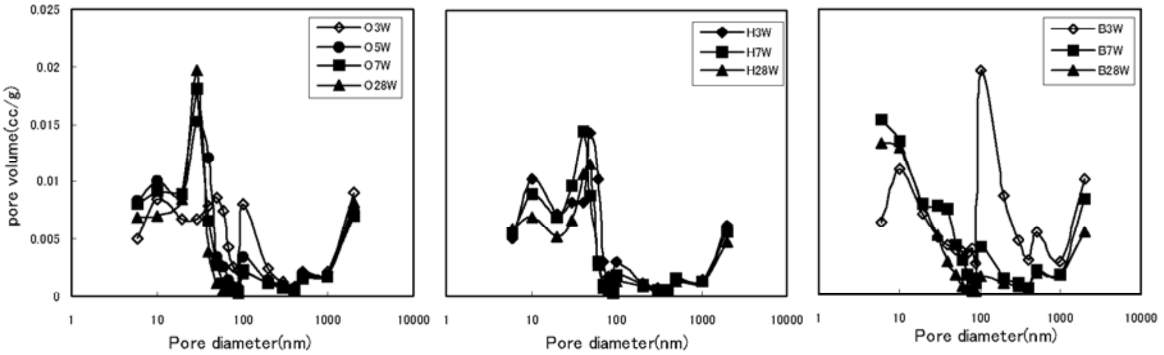

(a) OPC (b) HPC (c) BFS

Fig. 5 Pore size distribution by cement type

pores larger than 50 nm decreases significantly between 3 and 5 days and does not change significantly after 5 days. This indicates that there are differences in the formative period of pore structure according to the type of cement. The volume of each pore size range in the wet curing case is shown in Fig. 5 as a function of cement type. In the case of OPC, the 3-day-old specimen (O3W) shows a large volume of pores between 50 and 200 nm. For specimens with 5 days or more of curing (O5W, O7W, and O28W), although the distribution is slightly different, the results are similar and a peak is observed for pores in the 20-50 nm range. This demonstrates that the structure of OPC concrete is generally defined during wet curing from the age of 5 days. In the case of HPC, the pore structure is defined at 3 days (H3W) and the peak in pore volume does not change after 7 days (H7W) or 28 days (H28W). Conversely, at the age of 3 days BFS concrete (B3W) exhibits a porous structure and the peak is for pores of around 200 nm. The hydration of ground granulated blast-furnace-slag is very active for the first 7 days (B7W) and the volume of pores larger than 100 nm is low. In the period between 7 and 28 days, a similar tendency is observed and the peak of pore volume is 10 nm or less. Once BFS concrete is sufficiently cured, it has a nonporous pore structure.

The standard specifications of the JSCE recommend maintaining moist conditions for 5 days or more for OPC, 3 days or more for HPC, and 7 days or more for blended cement (Portland blast-furnace slag cement and Portland fly-ash cement). Considering the results shown in Fig. 5, it is reasonable to stipulate a standard curing period in this way.

3.2 Influence of drying

In order to investigate the influence of drying on pore structure, the pore size distribution during

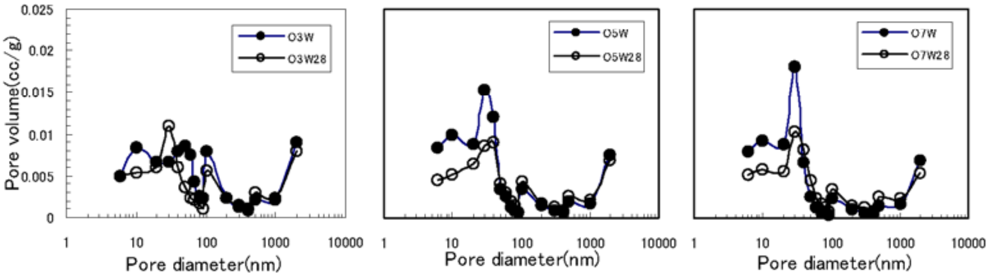

(a) OPC

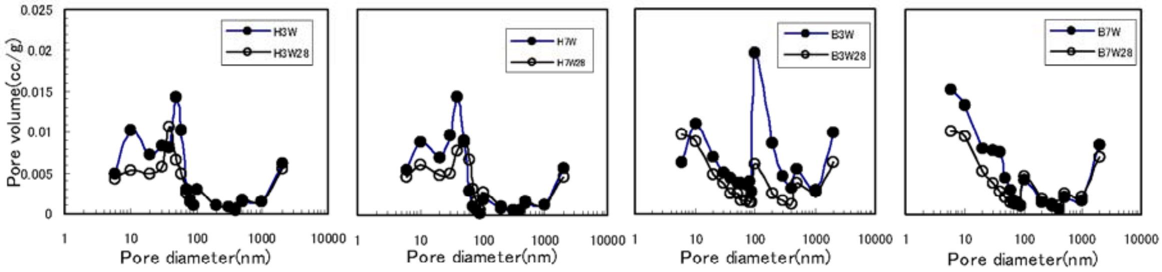

(b) HPC (c) BFS

Fig. 6 Variation in pore size distribution with drying

the prescribed wet curing period and on through continuous drying to a total of 28 days was measured. The results of this experiment are shown in Fig. 6. It is well known that a lowering of moisture content due to evaporation from the concrete surface limits hydration[7]. This means that air-drying after early wet curing will cause a change in the previously noted wet-curing behavior, in which the volume of pores measuring less than 200 nm decreases with time. As shown in Fig. 6, the pore structure of OPC concrete subjected to water curing is established after 5 days, and the volume of pores larger than 70 nm does not change significantly after this time. Also, it can be seen that the volume of pores smaller than 70 nm in HPC concrete decreases after 3 days and, as with OPC, that of BFS decreases after 7 days. If concrete is dried in air after initial wet curing, hydration only takes place in pores smaller than 70 nm because the moisture in relatively large pores is lost to the air by evaporation.

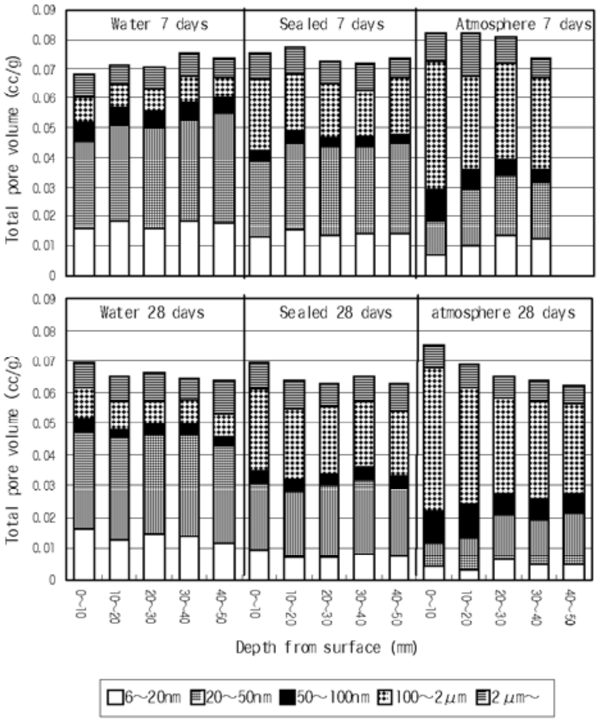

Fig. 7 Pore structure by curing conditions

Differences in pore structure with type of curing are illustrated in Fig. 7, where the pore volume of OPC samples at the age of 7 and 28 days is plotted against depth from the surface. Although there is no significant variation in total pore volume with type of curing, there is a clear difference in pore size composition, especially in the range 100 nm to 2 μm. It is well known that the pore size distribution, not the total pore volume, is the actual determinant of concrete strength, permeability, and volume change[8]. It can be seen that there are few pores larger than 50 nm in the case of concrete cured in water for

28 days, because in this case the cement obtains a sufficient supply of moisture for hydration. Conversely, in the case of samples that were air-dried for 7 days, the volume of pores larger than 50 nm accounts for a major portion of the total pore volume. The number of pores of this size decreases with depth, while there are more pores of 50 nm and over. That is, air curing leads to a loss of homogeneity in the depth direction. Only concrete in the vicinity of the surface is influenced by drying, whereas hydration tends to progress at greater depths. This behavior is more clearly seen at the age of 28 days. Water or sealed curing, which ensures a constant degree of moisture distribution, results in a homogeneous structure with regard to pore structure.

4. PORE STRUCTURE AND COMPRESSIVE STRENGTH

It is a well known there is an inverse relationship between porosity and strength[8]. Strength resides in the solid part of the concrete, and voids are detrimental to strength. Stress concentrations and subsequent rupture on application of load begin at large capillary voids and micro-cracks.

The relationship between strength and porosity can be observed in Fig. 8, where compressive strength after the prescribed curing period (3, 5, and 7days) and then drying until 28 days is plotted against total pore volume. Although the plotted data cover the relatively early age up to 28 days, there is good correlation between strength and total pore volume. It can be seen that compressive strength is ranked in the order BFS, OPC, and HPC.

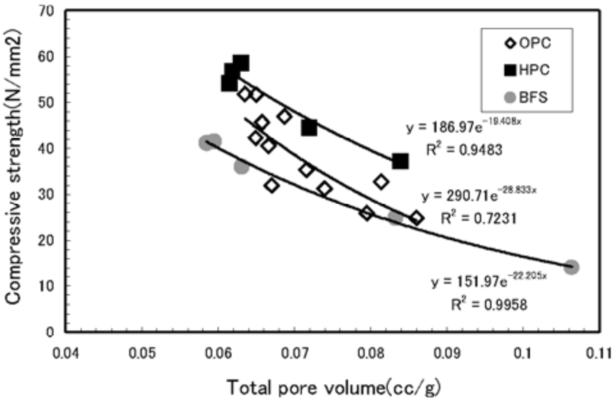

Fig. 8 Relationship between total pore volume and compressive strength

5. PORE STRUCTURE AND CARBONATION

5.1 Influence of pore size on carbonation

Figure 9 shows the results of accelerated carbonation tests on OPC concrete under different curing conditions. The volume of $Ca(OH)_2$ increases with hydration. The carbonation rate, or the rate at which the reaction of calcium hydroxide and carbon dioxide proceeds, falls with increasing curing time and with curing conditions ranked as air curing, sealed curing, then water curing.

Carbon dioxide may penetrate the concrete and diffuse inwards from the surface in a process that is dependent on the presence of capillary voids. Darr and Ludwig[9] showed that the diameter of gas bubbles that freely pass through concrete ranges from 50 to 100 nm. Although carbon dioxide travels freely within capillary voids, its diffusion is inhibited considerably by the presence of a water membrane. It should also be noted that the diffusion rate in a liquid is 10^{-3} times[10] or 10^{-4}-10^{-5} times[11] slower than in a gas.

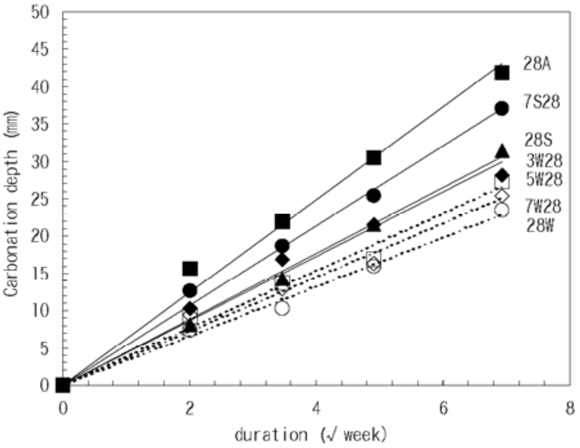

Fig. 9 Depth of carbonation

The equilibrium vapor pressure in a pore of given diameter can be determined from the radius of curvature of the liquid meniscus in the pore. This leads to the Kelvin equation:

$$\ln\frac{P}{P_0}=-\frac{2\gamma M\cos\theta}{RT\rho}\cdot\frac{1}{\mathrm{r}} \tag{1}$$

where P is the saturation vapor pressure of the bulk liquid, P the saturation vapor pressure of the liquid in a pore of diameter r, γ the interfacial (surface) tension of water (0.07336 N/m), M the molecular weight of water (0.01802 kg/mol), ρ the density of water (1,000 kg/m^3) T the absolute temperature, θ the angle of contact of water (0 degrees), and R the ideal gas constant (8.31441 J/mol・k). The condensing pore radius can be determined by substituting a temperature of 40℃ and a relative humidity of 50% into Equation (1). Condensing pores within the range of this experiment are pores smaller than 2.9 nm.

From the above, it is inferred that there is a critical pore size that affects the mechanism of carbonation. In order to determine this critical size, the relationship between relative pore volume ratio and relative carbonation ratio in each pore size range is plotted, as shown in Fig. 10. The relative pore volume ratio is defined as the ratio of pore volume in the reference specimen (the open circles in the graph) to that of the specimen in question, the reference specimen being O28W. In the same way, the relative carbonation ratio is the ratio of carbonation depth in the reference specimen to that in the specimen in question after 12 weeks in the accelerated carbonation chamber. Specimen O28W exhibited the lowest porosity and the slowest of rate of carbonation within the scope of this experiment.

Carbonation ratio increases with pore size. Nevertheless, the four graphs in the range from 6 to 40 nm show a decreasing trend. Sample O28W, which exhibited the slowest carbonation rate, has the greatest pore volume in this range. However, in the range above 40 nm, although it is not a clear tendency, these relative pore volume ratios are greater than O28W, as can be seen Fig. 10. In other words, the volume of pores measuring between 6 and 40 nm does not have a significant

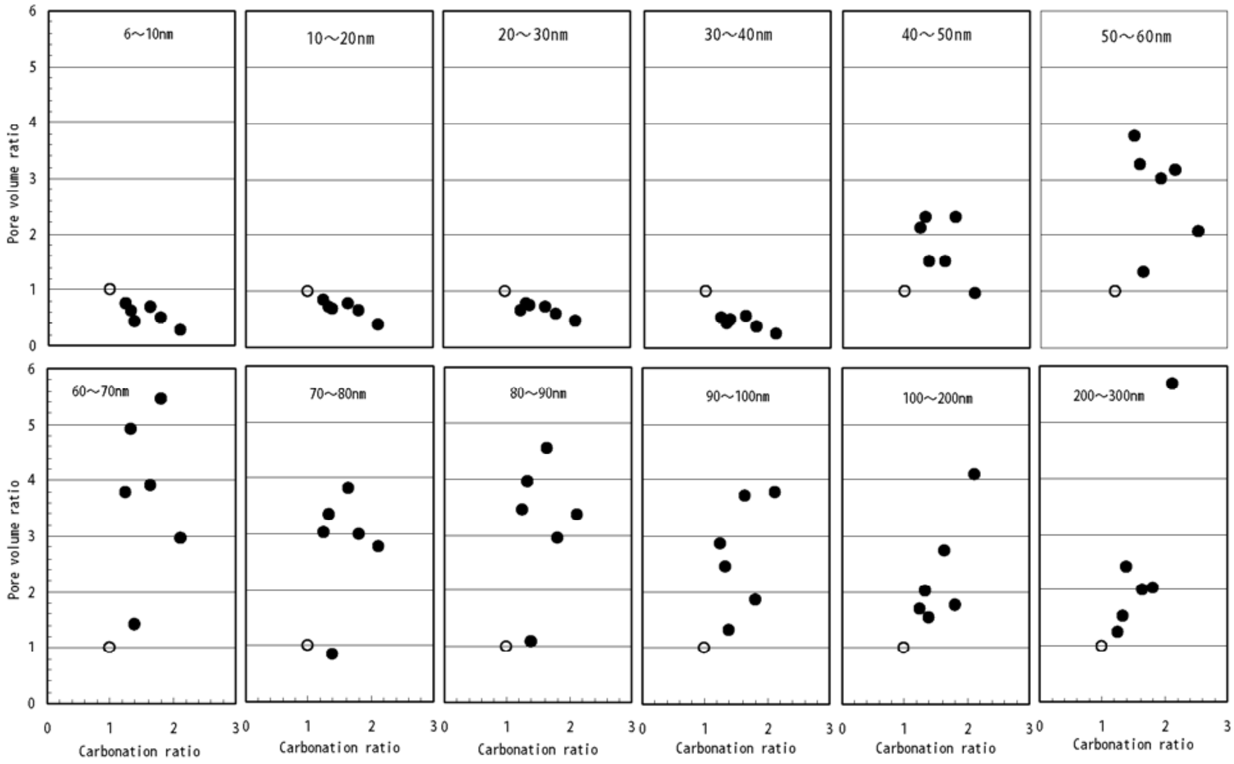

Fig. 10 Relationship between relative carbonation ratio and pore volume ratio

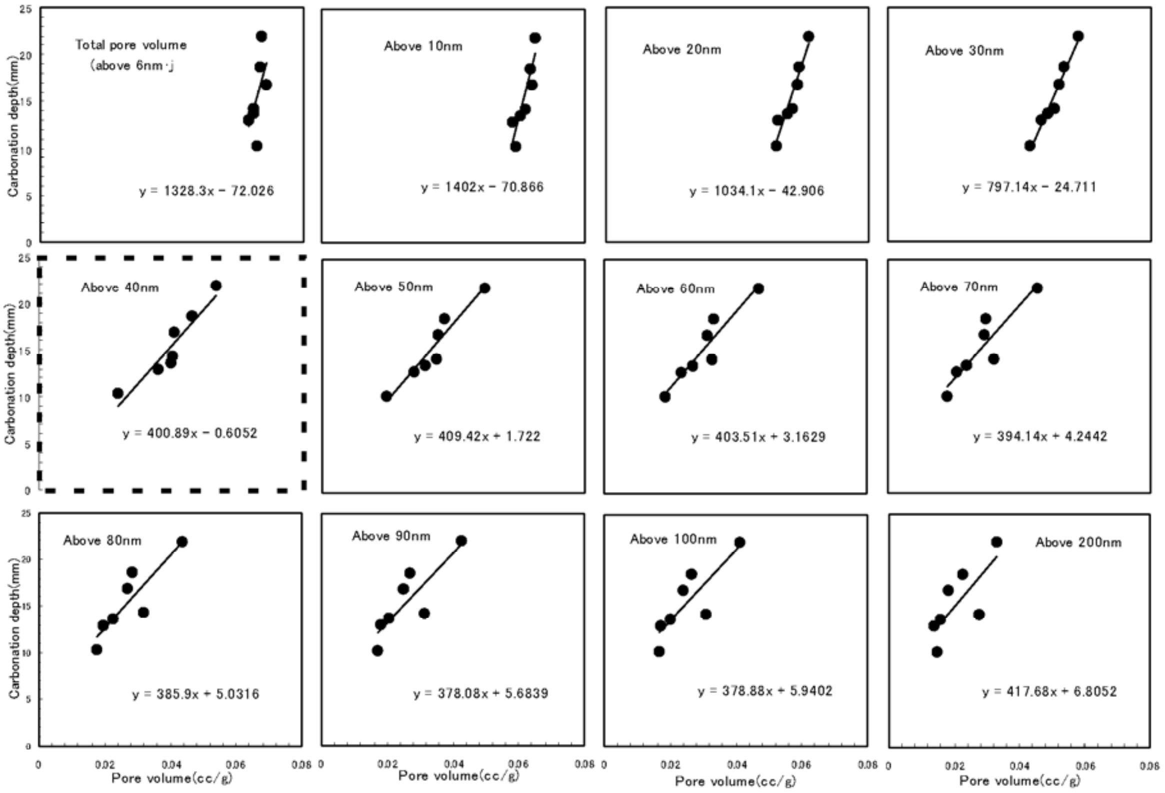

Fig. 11 Evaluation of critical pore size affecting carbonation

influence on carbonation rate.

The relationship between carbonation depth at the accelerated age of 12 weeks and pore volume is shown in Fig. 11. The second term of the empirical equation given in the graph is the Y-axis intercept. It seems reasonable to suppose that this intercept term reflects the influence of pores of sizes not represented in the graph. For instance, in the graph for volume of pores larger than 50 nm, the intercept on the Y-axis represents the influence of pores below 50 nm in size. Where the intercept is negative, this argument does not apply. So, since the intercepts of graphs for pore sizes 6 nm, 10 nm, 20 nm, and 30 nm are clearly negative, it is deduced that pores of sizes 6-40 nm do not have a significant influence on the carbonation process. In the case of pores larger than 40 nm, although the intercept is at -0.6052, this value may be within the range of error.

The value of the intercept increases with pore size. For example, the intercept is 1.722 at 50 nm and 3.1629 at 60 nm. This represents the varying degree of influence of pores between 50 nm and 60 nm. This investigation by means of linear approximation appears reasonable, and it shows that the volume of pores larger than 40 nm has a predominant influence on the carbonation process.

Figure 12 shows the relationship between the volume of pores larger than 40 nm and

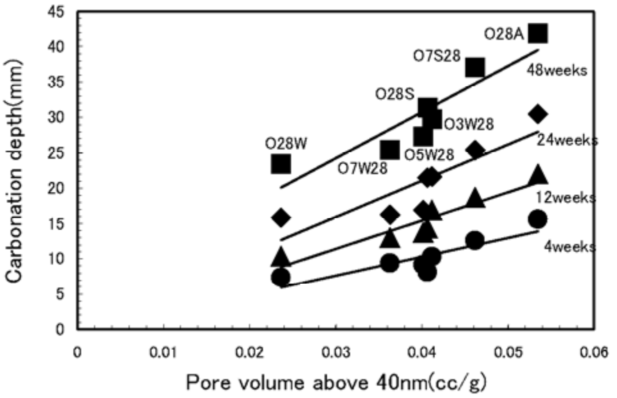

Fig. 12 Relationship between pore volume above 40nm and carbonation depth

accelerated carbonation depth at 4, 12, 24, and 48 weeks. For different curing conditions, the carbonation depth decreases in the order of air curing, sealed curing, and water curing. Carbonation depth also decreases with longer initial curing time. This is because the degree of hydration increases in the same order, and hence the volume of pores larger than 40 nm decreases. Although there is some scatter, an adequate correlation is obtained from Fig. 12, regardless of accelerated carbonation age.

5.2 Estimated carbonation rate

The carbonation rate is normally assumed to follow the relationship

$$X = b\sqrt{t} \tag{2}$$

Where X is carbonation depth, t is time, and b is a constant depending upon the mix proportion and environmental conditions. (This equation represents the slope of each line in Fig. 9. Although a large number of investigations of carbonation rate have been performed[12], little is known about the quantitative relationship between carbonation rate and curing conditions. For this reason, we attempt to estimate the carbonation rate by considering the variations in pore structure caused by curing conditions.

Any experimentally obtained carbonation rate will reflect the influence of cement type, water-cement ratio, curing conditions, exposure conditions, and so on. The pore size distribution also depends on cement type, water-cement ratio, curing conditions, etc. Therefore, pore size distribution has the potential for use as an index of carbonation, and may be appropriate for use in the estimation of carbonation rate.

Given that the volume of pores larger than 40 nm has a predominant influence on the carbonation process, we can derive the following relationship between carbonation rate and the volume of pores larger than 40 nm:

$$b = f(PV_{40}) \tag{3}$$

Where PV_{40} is the volume of pores larger than 40 nm. This relationship is expressed by the linear equation plotted in Fig. 13. An empirical equation can be obtained using the least squares method:

$$b = 101.78X + 0.3627 \tag{4}$$

where X denotes the volume of pores larger than 40 nm. Again, the Y-axis intercept can be taken to reflect the influence of pores smaller than 40 nm.

Figure 14 compares the test results of carbonation depth against estimated

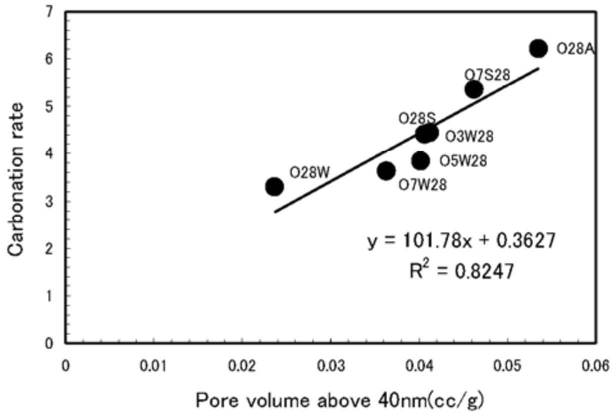

Fig. 13 Relationship between pore volume above 40nm and carbonation rate

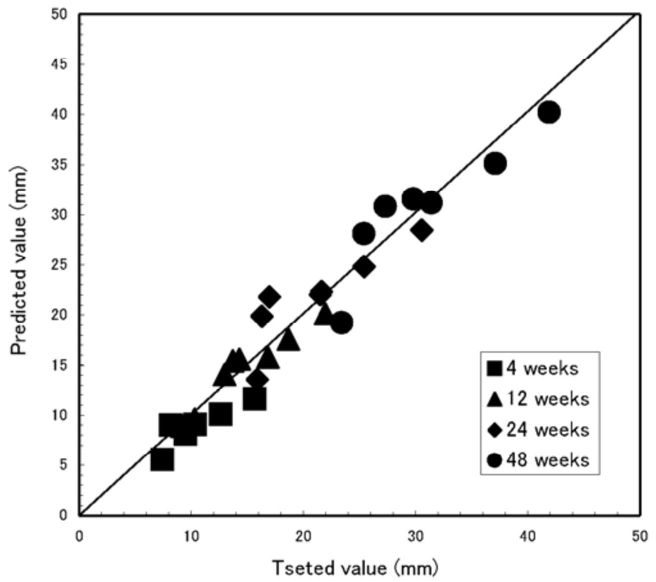

Fig. 14 Comparison of test results with calculated values of carbonation depth

values obtained using this equation. Although there is some scatter, the correlation is good overall, and does not depend on differences in curing conditions. This result clearly shows that it is possible to estimate carbonation rate on the basis of pore structure.

6. CONCLUSIONS

In this study, we investigated the variation of pore structure with depth under different curing conditions and the influence of pore structure on carbonation. The following conclusions were reached through the study:

(1) Wet curing yields a homogeneous pore structure. Atmospheric curing leads to inhomogeneity as a result of the non-uniform moisture distribution with respect to depth.

(2) Variations in pore structure due to hydration occur mainly in pores smaller than 200 nm. There is no significant decrease in the volume of pores larger than 200 nm as hydration proceeds.

(3) There are differences in the period during which the pore structure is formed according to type of cement. In terms of pore structure, the standard curing periods stipulated in the JSCE specifications are reasonable.

(4) The volume of pores larger than 40 nm has a predominant influence on the carbonation process. Carbonation depth exhibits a linear relation with the volume of pores larger than 40 nm, regardless of curing conditions.

(5) Given this linear relationship between carbonation depth and pore volume, it is possible to estimate carbonation rate from information on the pore structure.

REFERENCES

[1] Japan Society of Civil Engineering, Standard specifications for concrete structures [constructions], 1999 (in Japanese)
[2] Doyeon, K., Uji, K., Kokubu, K., and Ueno, A., "Inhomogeneity of pore structure due to drying on the concrete", Proceedings of the JCI, Vol.24-1, pp.711-716, 2002.6 (in Japanese)
[3] Yuasa, N., Kasai, Y., and Matsui, I., "Inhomogeneous Distribution of the Moisture Content and Porosity from the Surface Layer to Internal Parts of Dried Concrete", J. Struct. Constr. Eng., AIJ, No.509, pp.9-16, 1998.7 (in Japanese)
[4] Doyeon, K., Uji, K., Kokubu, K., and Ueno, A., "Variation of Pore Structure According to Cement and Curing Conditions", Proc. of the 54th JSCE annual convention, pp.580-581, 2001.10 (in Japanese)
[5] Saeki, T., Ohga, H., and Nagataki, S., "Change in Micro-Structure of Concrete due to Carbonation", Journal of Materials, Concrete Structures and Pavements, No.420/V-13, pp.33-42, 1990.8 (in Japanese)
[6] Kokubu, K., Murata, Y., Takahashi, S., and Anzai, H., "Studies on Adiabatic Temperature Rise and Hydration of Portland Cement Concrete Incorporating Ground Granulated Blast Furnace Slag", Journal of Materials, Concrete Structures and Pavements, No.369/V-9, pp.39-48, 1988.8 (in Japanese)
[7] Iyoda, T., and Uomoto, T., "Progress of Hydration and Amount of Free Water in Hydrated Cement in Arid Condition Continuously on Early Curing", Cement Science and Concrete Technology, No.54, pp.167-173, 2000 (in Japanese)
[8] P. Kumar Metha and Paulo J.M Monteiro: CONCRETE—Microstructure, Properties and Materials—, The McGRAW-Hill Companies, INC., pp.28, pp44, 1985
[9] Darr, G.M., and Ludwig, U., "Determination of Permeable", Materials and Structures, Vol.6, No.33, pp.185-190, 1973
[10] Ying-yu, L., and Qui-dong, W., "The Mechanism of Carbonation of Mortar and the Dependence of Carbonation on Pore Structure", Proceedings of the Katharine and Bryant Mather International Conference on Concrete Durability, ACI SP100-98, pp.1915-1943, 1987

[11] Lawrence, C.D., “Transport of Oxygen through Concrete”, Proceedings of Concrete Society, Meeting on Chemistry and Chemically-Related Properties of Cement, Imperial College, London, pp.277-293, 1984

[12] Nagataki, S., Mansur, M.A., and Ohga, H., “Carbonation of Mortar in Relation to Ferrocement Construction”, ACI Materials Journal, pp.17-25, 1988.1-2

[13] Uchikawa, H., Hanehara, S., and Sawaki, D., “Estimation of the Thickness of Transition Zone in Hardened Mortar and Concrete, and Investigation of the Relationship between their Thickness and Strength Development”, Concrete Research and Technology, JCI, Vol.4, No2, pp.1-8, 1993.7 (in Japanese)

[14] Sidney, D., “Mercury porosimetry an inappropriate method for the measurement of pore size distributions in cement-based materials”, Cement and Concrete Research 30, pp.1517-1525, 2000